International Journal of Automotive and Mechanical Engineering
ISSN: 2229-8649 (Print); ISSN: 2180-1606 (Online)
Volume 16, Issue 1 pp. 6402-6414 March 2019

Finite Element Simulation of Equal Channel Angular Pressing: Effect of Die Angle and Number of Passes

D. N. Awang Sh'ri [1*], M. A. H. Abu Hassan[1,2], Z. S. Zahari[1,2] and W. S. Wan Harun[1]

[1]Human Engineering Group, Faculty of Mechanical Engineering, Universiti Malaysia Pahang, 26600 Pekan, Pahang, Malaysia
[*]Email: noorfazidah@ump.edu.my
Phone: +6094246311; Fax: +6094246222
[2]Institute of Postgraduate Studies, Universiti Malaysia Pahang, Lebuhraya Tun Razak, 26300 Gambang, Kuantan, Pahang, Malaysia

ABSTRACT

Equal channel angular pressing (ECAP) is one of the popular severe plastic deformation processes used to produce bulk nanostructured materials. The degree of homogeneity of nanostructured is affected by various die parameters. In this paper, the effect of internal die angle (ϕ) and number of passes (N) on the strain behaviour of Aluminium Alloy 6061 (AA6061) during ECAP was investigated by using three-dimensional finite element analysis. The effect of number of passes and die angle on the homogeneity within the workpiece was analysed in terms of contours, radial view contour and inhomogeneity index. The analysis is done by comparing workpiece extruded up to 8 passes at die angle of 120° and 126°. It is observed that the resulting strain is higher at 120° die. However, the inhomogeneity index is decreasing in a similar pattern in both dies. The simulation results shed some lights on the optimum design of ECAP die for homogeneous microstructure.

Keywords: Equal channel angular pressing (ECAP); bulk nanostructured metals, severe plastic deformation; aluminium alloy 6061.

INTRODUCTION

Equal channel angular pressing (ECAP) is one of the most popular methods that is related to the investigation in severe plastic deformation (SPD). It was first developed by Segal [1, 2], and later improved by Ruslan Valiev [3–5]. In the ECAP process, the sample will be pressed through an angular channel with the same cross-sectional area under high extreme high shear strain. The principle of ECAP process is to produce bulk nanostructured materials with ultra-fine grain (UFG) with same cross section after pressing process, by allowing the process to be repeated for multiple passes to produce a sample with desired mechanical properties. The equivalent shear strain can be measured by using Eq. (1) where *(N)* is the number of passes, and *(ϕ)* is the internal angle as indicated in Figure 1 [6].

$$\varepsilon_N = \frac{2N}{\sqrt{3}} \cot\left(\frac{\Phi}{2}\right) \quad (1)$$

Subsequently, Iwahashi et al. [7] modified the above equation to include the external angle (Ψ), which is given as

$$\varepsilon_N = \frac{N}{\sqrt{3}}\left[2\cot\left(\frac{\Phi}{2}+\frac{\Psi}{2}\right)+\Psi\cdot\csc\left(\frac{\Phi}{2}+\frac{\Psi}{2}\right)\right] \quad (2)$$

Eq. (1) and (2) emphasises on the effect of die angle and number of passes as the important parameters in ECAP process that affecting the effective strain [8]. These equations show that by lowering the angles, the strain per pass imposed on the samples will increase. The strain is also increasing as the number of passes increases. However, as strain magnitude getting higher, the distribution of the strain across the samples may be compromised. The pressing force required also may increase with lower angle [9].

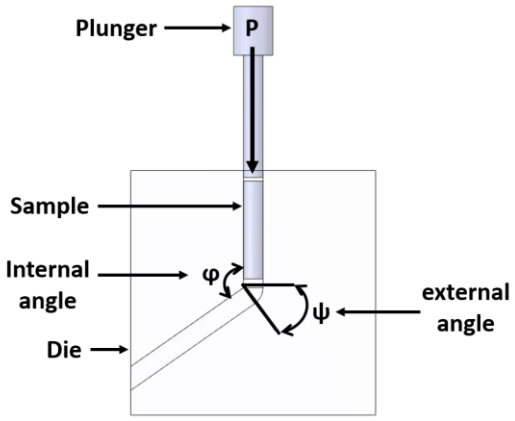

Figure 1. The schematic illustration of the ECAP process.

Finite element analysis (FEM) has been used for analysis on strain distribution, strain inhomogeneity [10], and the peak pressure required for pressing. In the ECAP process, most of the FEM analysis done to analyse the deformation behaviour and the strain behaviour on the materials [9, 10]. This includes the effect of friction on the material movement [11], the type of material used [12–14], the effect of using back pressure to the process [15], and the strain localisation achieved in the sample under several parameters [16]. In recent years, there are FEM studies involving strain distribution and deformation distribution [17]. However, there are no study that investigate the effect of die angle and number of passes simultaneously. Therefore, the effect of these parameters on the strain distribution and strain homogeneity has been conducted in the present study. To avoid extensive parametric studies, this paper will focus only on the resulting effective strain distribution.

EXPERIMENTAL PROCEDURE

Experimental Detail

AA6061 rod with 10 mm diameter and 15 cm length, heat treated to a T6 condition, was used as the sample in this work. The ECAP die was built in-house with interchangeable die slot with two channels, equal in cross-section, intersecting at an angle near the centre of the die. Two different dies with channel angles of 120º and 126º respectively was used in this work. To reduce the friction between the rod and the die walls, a lubricant with

molybdenum disulfide (MoS_2) was used. A hydraulic press machine was used to carry out the ECAP process at room temperature.

The ECAP-processed specimens' hardness was investigated using Wilson Vickers hardness machine on the specimens that undergo only one pass. The specimens were subjected to a load of 100 gf for 10 seconds. The testing taken from 3 points horizontally and 7 points vertically to check the hardness distribution across the samples. Each point in each group located 1 mm from another point horizontally. Figure 2 shows the hardness testing distribution points used in this study.

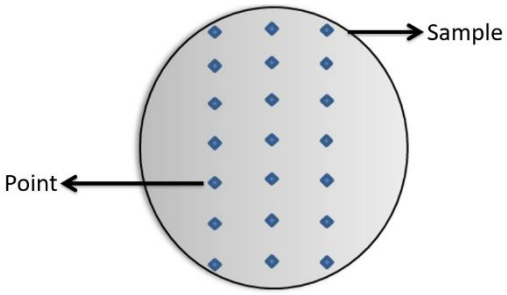

Figure 2**.** Hardness testing distribution points.

Finite Element Analysis

The simulation was carried out using Abaqus CAE. The die, as shown in Figure 3, was assumed as rigid to avoid any deformation and was set as fixed to avoid any movement occurred to it. There were two sets of the rigid die used in the analyses; each has the internal angle (ϕ) of 120° and 126°, while both external angles are 20°. The curve radius (r) for both dies is 10 mm. The sample was aluminium alloy 6061 in a cylindrical shape with a diameter of 9.8 mm and length of 50 mm. A finer mesh was applied at the channel of the die to achieve a smoother curve and produce more accurate simulation result. The mesh convergence has been performed to find the optimum number of elements for the sample. The optimum number of elements for the mesh is 2322 and non-linear geometric setup was turned on to accommodate the large deformation during the analyses. The sample was located closely before reaching the curvature of the die to decrease the time taken in the simulation analyses. The contact between the sample and the die were defined as general contact with the friction coefficient of 0.01 for all simulations. The simulation was done for eight passes by using route *A* for both set of die. The sample input for the property were; mass density is 2.7×10^{-9} tonne/mm; the modulus of elasticity is 7000 MPa; and the Poisson's ratio is 0.33 while yield strength and plastic strain is taken from true stress-strain curve of AA 6061 from Adnan N. Abood et. al. [18]. The resulting yield strength and plastic strain from each pressing was carried forward to the consequent passes, but the other parameter was kept as constant throughout the processes.

The pressure has been set at 77 MPa throughout the simulation. The time step was set at 0.0025 to reduce the time taken and to produce more accurate animation. The simulation was set to run at room temperature. The effect of die angle and the number of passes has been investigated on the strain behaviour of the sample with a total of 16 runs. The results for the equivalent plastic strain (*PEEQ*) are calculated. The equivalent plastic strain is recorded at certain element for nine points as in Figure 4. The radial view is taken at approximately 4 mm from the bent for every process to provide more precise strain value to the specific location of the sample.

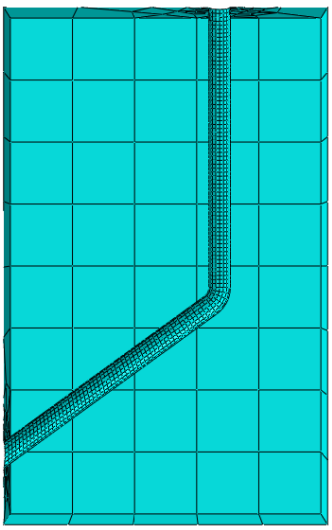

Figure 3. The view cut meshed 120° ECAP die.

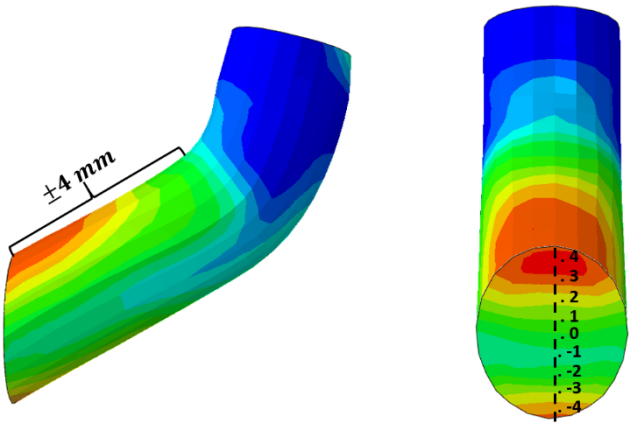

Figure 4. The locations of the point used for analysis in the vertical centerline at the transverse direction of the sample.

RESULT AND DISCUSSION

Effect of Die Angle and Number of Press to PEEQ

To understand the simultaneous effect of die angle and number of presses to the strain distribution, the simulation results for the equivalent plastic strain distribution in the pressed samples are shown in Figure 5 for 120° and Figure 6 for 126°. Based on Figure 5 and 6, both sets of die managed to perform strain hardening to the sample.

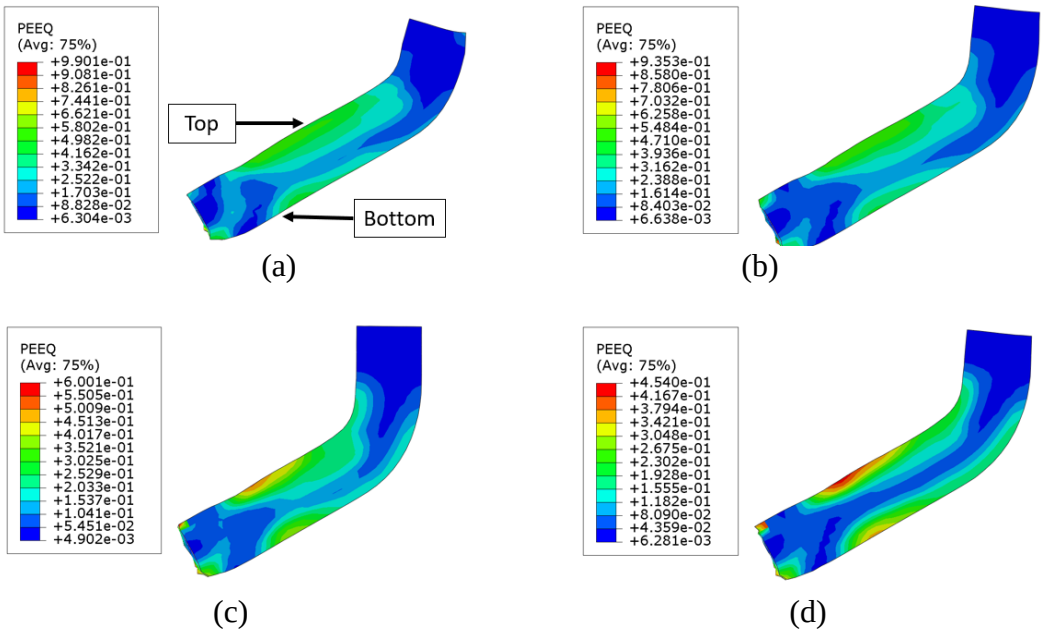

Figure 5. The view cut of *PEEQ* of 120° for: (a) first pass; (b) second pass; (c) fourth pass; (d) eighth pass.

At the first pass, as shown in Figure 5(a), non-uniformed strain distribution is observed with more strain accumulated at the top of the samples upon pressing. As the number of pass increases, as indicated in Figure 5(b) to 5(d), the strain distribution gets more homogeneous throughout the sample even though higher strain magnitude is recorded on the top of the sample.

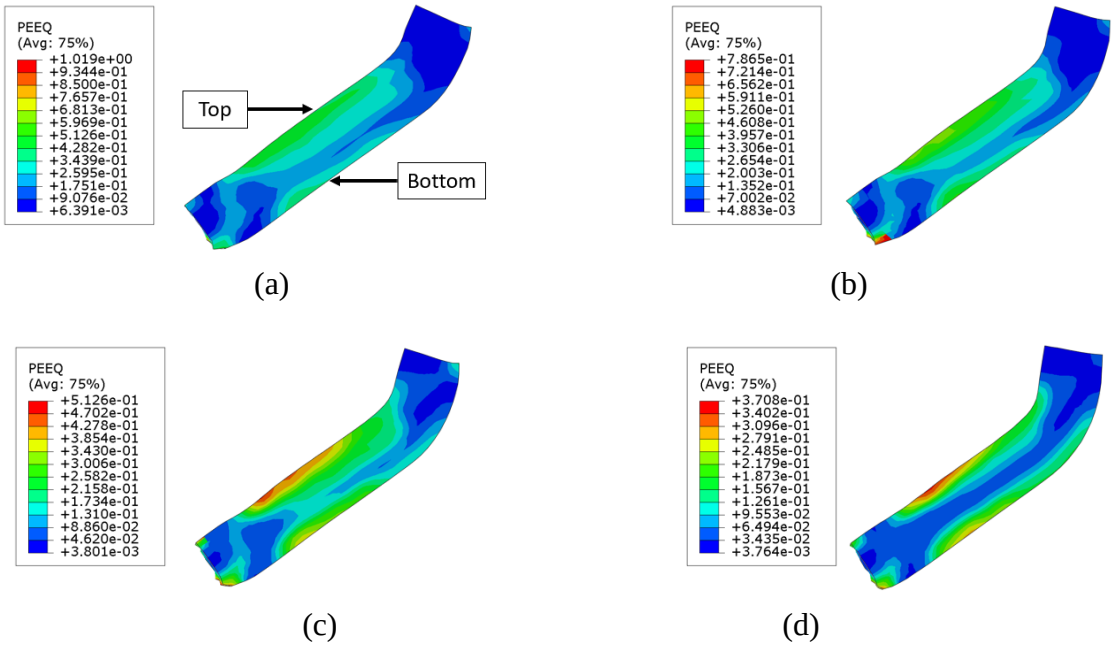

Figure 6. The view cut of *PEEQ* of 126° for: (a) first pass; (b) second pass; (c) fourth pass; (d) eighth pass.

A similar trend was observed in samples in 126° die shown in Figure 6. However, the strain value for 126° die is lower than 120° die. Moreover, the strain distribution is more homogeneous throughout the sample at 126° die. This result is also supported by Patil et al. [19] where he found that in strain hardening process, the strain value is decreasing as the angle of the die increased. The degree of inhomogeneity can be summarised by using

$$\varepsilon_i = \varepsilon_{max} / \varepsilon_{min} \quad (3)$$

where the ε_{max} is the maximum strain recorded at current press while ε_{min} is the minimum strain recorded. From the Eq. 3, the degree of inhomogeneity for both dies is illustrated in the Figure 7. Both set of die angles started at approximately 1.6 % and then decreased to 0.7 % for 120° die and 1.0 % for 126° die. The trend for 120° die showed it decreased across the pressing process while for 126° die, it showed that a linear percentage in the second pass but decreased at the fourth and final pass. The percentage of inhomogeneity for 120° die is lower compared to 126° die. Nevertheless, the trend for the degree of inhomogeneity proved that the strain distribution for both dies does become more homogenous as the number of press increased.

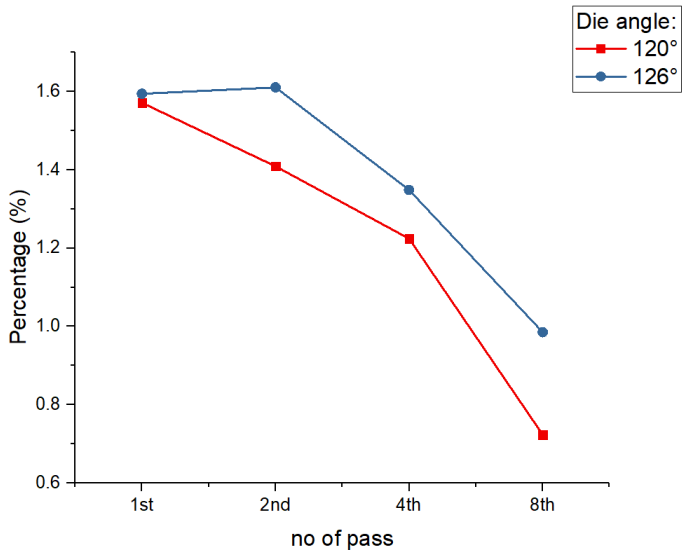

Figure 7. The percentage of degree of inhomogeneity under ECAP process.

Figure 8 and 9 shows the strain in radial view for 120°, and 126° dies, respectively. In the radial view of the sample, the variation of strain distribution can be seen starting from the top to the bottom section of the sample, which indicated that strain hardening mechanism phenomenon took place in the process. The variation strain value in the sample showed that the highest strain value is located at the top of the sample. The reading value was found to be decreasing as it moved to the middle of the sample but increased back as it moved to the bottom of the sample. According to Figure 8 and Figure 9, the dark red region (indicated the highest strain) is getting smaller as the number of passes increased. It can be interpreted that the microstructure stopped to recrystallize. The strain from the earlier passes has fragmented the grains into a smaller size. However, at the final pass, the fragmented microstructure size is more homogenous throughout the sample. Thus, the strain value is becoming lower than its previous pass and the effect of grain

refinement can be neglected. The trend for 126° die showed the same as the 120° die but has lower strain value compared to 120° die.

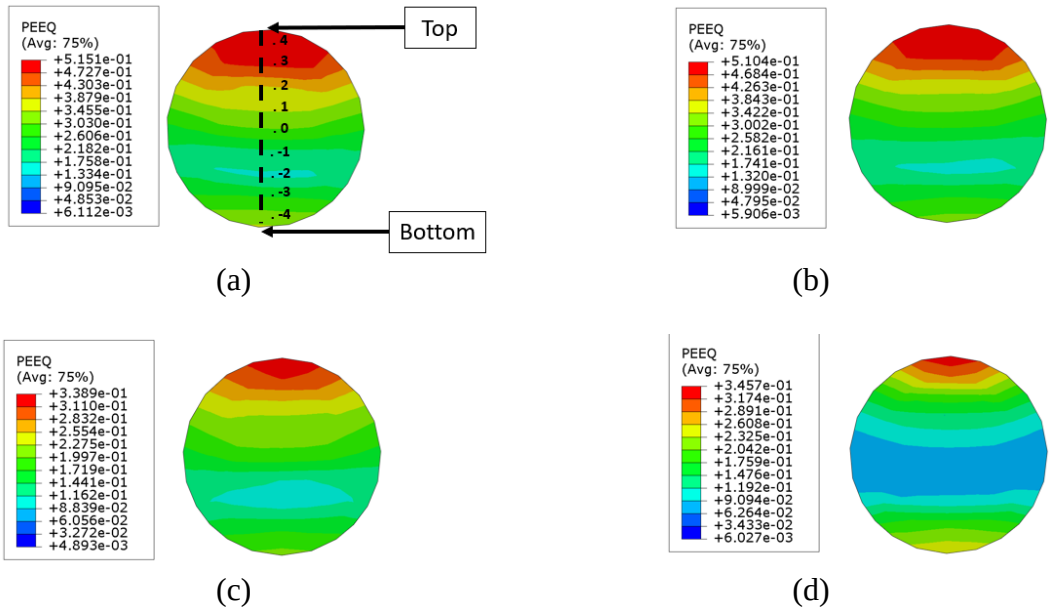

Figure 8. The radial view of *PEEQ* of 120° for: (a) first pass; (b) second pass; (c) fourth pass; (d) eighth pass.

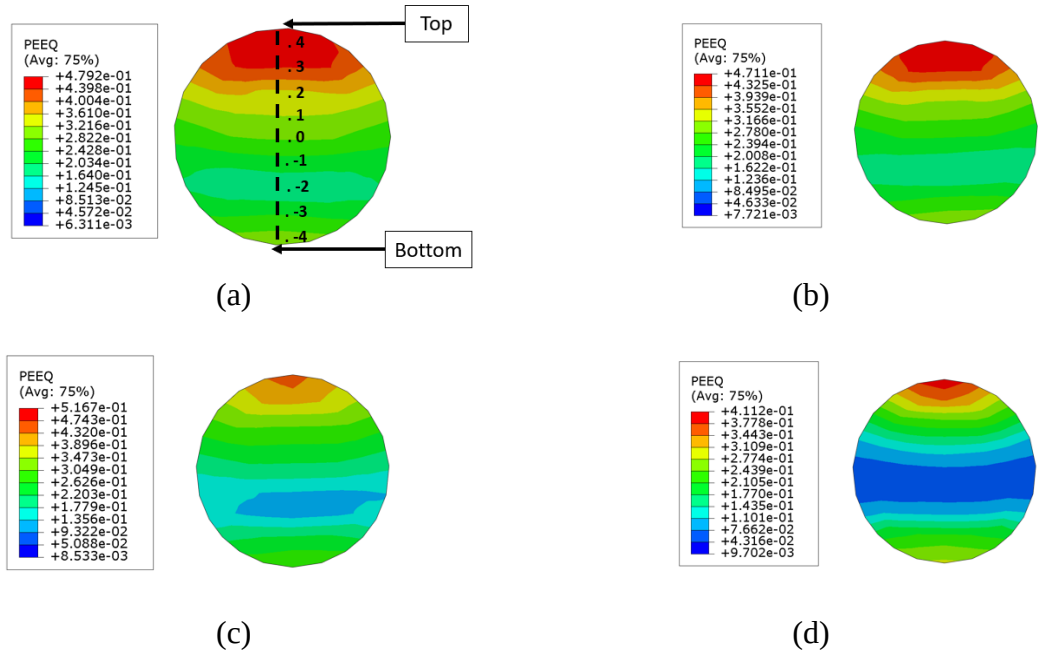

Figure 9. The radial view of *PEEQ* of 126° for: (a) first pass; (b) second pass; (c) fourth pass; (d) eighth pass.

Figure 10 shows the percentage of degree of inhomogeneity for both dies in term of radial view of the samples. The degree of inhomogeneity in this part is more precise since it focused on a certain part of the samples. The same equation as in Eq. (3) is used to obtain the percentage of degree of an inhomogeneity. Based on Figure 10, the degree

of inhomogeneity decreased throughout the pressing process. At the first pass, the percentage of inhomogeneity for 120° and 126°dies were found to be at 0.84 % 0.76 %, respectively. At the final pass, the percentage of inhomogeneity has decreased to 0.57 % for 120° die and decreased to 0.42 % for 126° die. The trend for 120° die is maintained at the second pass but eventually decreased throughout the presses. For the 126° die, the strain decreased on the second pass and maintained to the fourth pass but decreased during the eighth pass. The trend for inhomogeneity index in radial view for both angles are similar to the strain inhomogeneity shown in Figure 7. Since the strain inhomogeneity at the radial view is the same as the whole view, it is proved that the strain distribution is becoming more homogenous throughout the passes even at all-region in the sample.

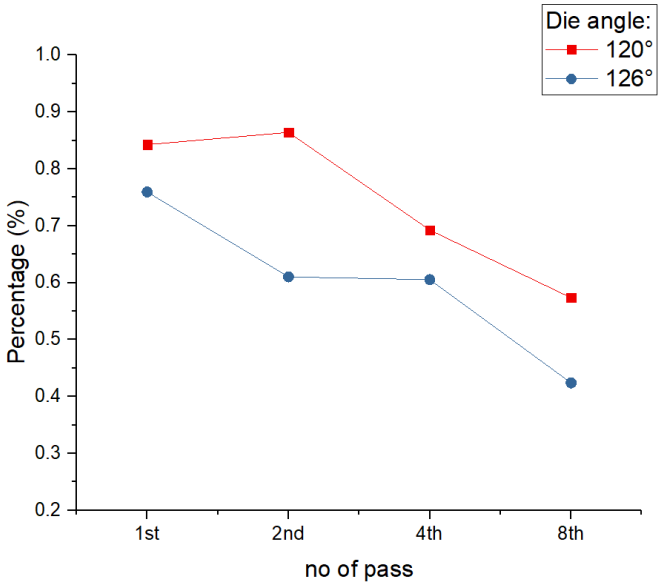

Figure 10. The percentage of degree of inhomogeneity under ECAP process at the radial view.

The difference in strain distribution on the top and bottom of the samples can be attributed to the effect of the die corner. As AA6061 is typically behaving as a quasi-perfect plastic material, the workpiece deforms as the ram presses, and the die corner is filled with the top part of the sample. The bottom surface of the samples goes through shorter distance; thus the bottom surface of the samples experiences lower shear deformation compared to the top surface [20]. The similar trend also was observed in previous works with 3D FEM simulation [21, 22]. The effect of number of passes on the strain behaviour can be explained by microstructural evolution of ECAP-ed material. At first pass, the pure shear deformation causes grain elongation and high angle grain boundary formation. At further pressing, the strain induced during deformation increases the dislocation density leading to the formation of subgrain. Higher fraction of high angle grain boundary starts to form and microstructural homogeneity is achieved [23].

The *PEEQ* at the same location used in radial view for each pass is shown in Figure 11. The overall trend showed that the strain is decreasing as the number of passes increased although the strain increased in the final pass for 120° die. There is different observation for 126° die, in which the strain decreased as the number of passes increased up to the sixth pass. However, the strain value in the seventh and final pass is becoming homogenous across the sample pressed in 126° die. The same cannot be seen at the strain

value of the seventh and final pass for 120° die. The initial increase may be due to the simple shear deformation. The strain behaviour at the cross-section of the ECAP-ed samples has recorded the same results by several papers [24–26]. Djavanroodi et al. [27], observed the same phenomena in which the strain is increased but eventually reaching to a constant value when the reading of the sample is divided into three parts. However, the strain is increasing back starting from the seventh to the final pass. Based on the strain readings, it can be stated that the samples are undergoing dynamic recrystallisation period from the second to sixth pass. The same result has also been recorded by Y. W. Tham et al. [28] where the effective plastic strain of commercially pure Al showed a sudden increase at 8th passes even though initially the strain decreases with the number of press. As the strain increases, the recrystallisation phenomenon has stopped due to dislocation density and the microstructure has achieved ultra-fined grain. The trend for the strain is the same for both dies but the value of strain recorded is lower on the 126° pass compared to the 120° die. The strain recorded highest in the 120° compared with 126° at every point of the sample due to the extreme curvature at 120° die. To this effect, it can be stated that it is more difficult to press for 120° compared to 126° die.

Figure 12 shows the plot of the microhardness analysis for all the samples after one pass. The hardness gradient across the cross-section of the AA6061 bars is showing higher magnitude at the top end of the samples with lower hardness is observed at the centre of the samples. The hardness value is higher in samples that undergo ECAP in 120° die. The hardness and strain can be related to power law used to describe the hardening during ECAP.

$$HV = HV_0 + K\varepsilon_T^n \quad (4)$$

where ε_T is the true strain and HV_0, K and n are materials properties [29].

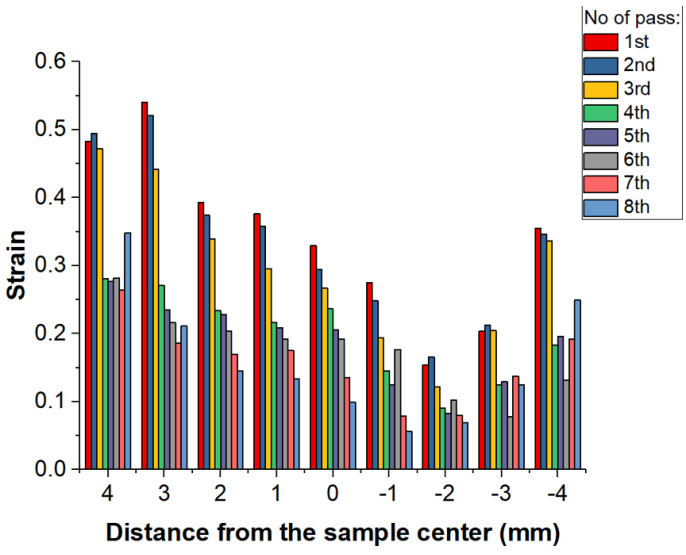

(a)

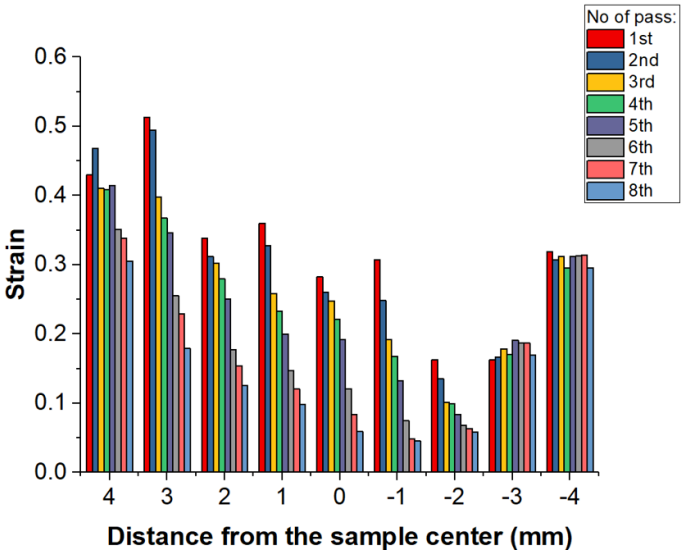

(b)

Figure 11. The graph of max *PEEQ* for every pass at a specific point for (a) 120° die; and (b) 126° die.

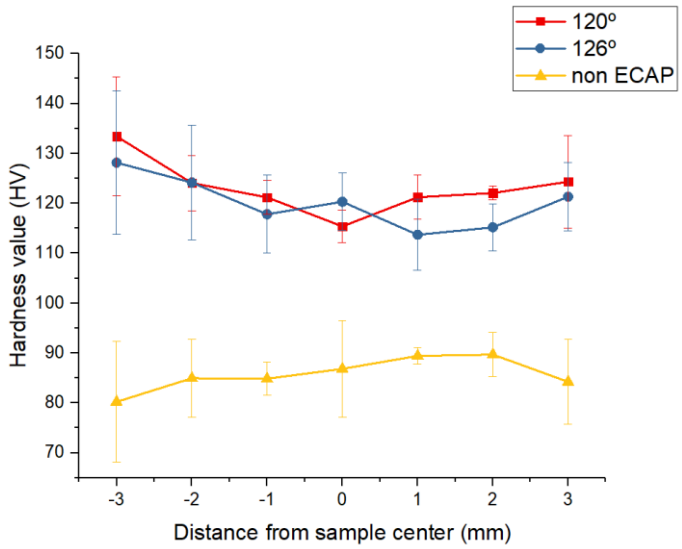

Figure 12. Vickers hardness profile across sample between non-ECAP and ECAP at die angle of 120º and 126º.

Thus, the trend in microhardness profiles in Figure 12 is in good agreement to the strain distribution shown in both Figure 7 and 8. The inhomogeneity of hardness profile and strain distribution is attributed to the pure bulk shear deformation during ECAP process and contribution of the convolution of the friction effects [30]. However, the observation in Figure 12 suggested that the hardness distribution of 120º sample was less homogenous compared to 126º, even though its average hardness is higher. Therefore, increasing the die angle can lead to a decrease in strain magnitude but the strain induced is more homogeneous throughout the samples [31].

CONCLUSION

The stress and strain behaviour for aluminium alloy 6061 under ECAP process was investigated by using 3D FEM analyses. From the studies, the following conclusion was drawn:

i. The effective strain imposed on the workpiece is influenced directly by the die angle. The value of equivalent plastic strain is lower when the angle of the die increased. However, the workpiece in 120° die is more difficult to press due to its smaller angle compared to 126° die.

ii. The strain distribution is more homogenous as the number of presses increased by measuring the degree of inhomogeneity. The degree of inhomogeneity for 126° die was found to reach a steady state after the fourth pass while it continues to decrease for 120° die.

ACKNOWLEDGEMENT

This paper was fully supported by facilities and resources from Universiti Malaysia Pahang. The author would like to acknowledge the support of a grant from Universiti Malaysia Pahang No. RDU180318 and Fundamental Research Grant Scheme, Ministry of Higher Education, Malaysia No. RDU190110.

REFERENCES

[1] Segal VM. Equal channel angular extrusion: from macro mechanics to structure formation. Materials Science and Engineering: A, 1999;271(1):322–33.

[2] Ferrasse S, Segal VM, Alford F, Kardokus J, Strothers S. Scale up and application of equal-channel angular extrusion for the electronics and aerospace industries. Materials Science and Engineering A, 2008;493(1–2):130–40.

[3] Valiev RZ. The new trends in fabrication of bulk nanostructured materials by SPD processing. Journal of Materials Science, 2007;42(5):1483–90.

[4] Valiev RZ, Estrin Y, Horita Z, Langdon TG, Zehetbauer MJ, Zhu Y. Producing Bulk Ultrafine-Grained Materials by Severe Plastic Deformation: Ten Years Later. The Journal of The Minerals, Metals & Materials Society, 2016;68(4):1216–26.

[5] Valiev RZ, Islamgaliev RK, Alexandrov IV. Bulk nanostructured materials from severe plastic deformation. Progress in Materials Science, 2000; 45: 103-189.

[6] Iwahashi Y, Horita Z, Nemoto M, Langdon TG. The process of grain refinement in equal-channel angular pressing. Acta Materialia, 1998;46(9):3317–31.

[7] Iwahashi Y, Wang J, Horita Z, Nemoto M, Langdon TG. Principle of equal-channel angular pressing for the processing of ultra-fine grained materials. Scripta Materialia, 1996;35(2):143–6.

[8] Iwahashi Y, Horita Z, Nemoto M, Langdon TG. An investigation of microstructural evolution during equal-channel angular pressing. Acta Materialia, 1997;45(11):4733–41.

[9] Sordi VL, Mendes Filho AA, Valio GT, Springer P, Rubert JB, Ferrante M. Equal-channel angular pressing: influence of die design on pressure forces, strain homogeneity, and corner gap formation. Journal of Materials Science, 2016;51(5):2380–93.

[10] Patil B V., Chakkingal U, Prasanna Kumar TS. Effect of geometric parameters on strain, strain inhomogeneity and peak pressure in equal channel angular pressing –

A study based on 3D finite element analysis. Journal of Manufacturing Processes, 2015;17:88–97.

[11] Kumar P, Panda SS. Finite element analysis of die angle at constant offset length in two-turn ECAP. IOP Conference Series: Materials Science and Engineering, 2016;149:012139.

[12] Esmaeili A, Shaeri MH, Noghani MT, Razaghian A. Fatigue behavior of AA7075 aluminium alloy severely deformed by equal channel angular pressing. Journal of Alloys and Compounds, 2018;757:324–32.

[13] Ashrafizadeh SM, Eivani AR, Jafarian HR, Zhou J. Improvement of mechanical properties of AA6063 aluminum alloy after equal channel angular pressing by applying a two-stage solution treatment. Materials Science and Engineering A, 2017;687:54–62.

[14] Koizumi T, Kuroda M. Materials Science & Engineering A Grain size effects in aluminum processed by severe plastic deformation. Materials Science & Engineering A, 2018;710:300–8.

[15] Shen J, Gärtnerová V, Kecskes LJ, Kondoh K, Jäger A, Wei Q. Residual stress and its effect on the mechanical properties of Y-doped Mg alloy fabricated via back-pressure assisted equal channel angular pressing (ECAP-BP). Materials Science and Engineering A, 2016;669:110–7.

[16] Horn T, Silbermann C, Ihlemann J. FE-Simulation based analysis of residual stresses and strain localizations in ECAP processing. Proceedings in Applied Mathematics and Mechanics 2017;17(1):309–10.

[17] Bylya OI, Sarangi MK, Ovchinnikova N V, Vasin R a, Yakushina EB, Blackwell PL. FEM simulation of microstructure refinement during severe deformation. IOP Conference Series: Materials Science and Engineering 2014;63:012033.

[18] Abood AN, Saleh AH, Abdullah ZW. Effect of Heat Treatment on Strain Life of Aluminum Alloy AA 6061. Journal of Materials Science Research. 2013;2(2):51–9.

[19] Patil Basavaraj V, Chakkingal U, Prasanna Kumar TS. Study of channel angle influence on material flow and strain inhomogeneity in equal channel angular pressing using 3D finite element simulation. Journal of Materials Processing Technology, 2009;209(1):89–95.

[20] Kim HS, Seo MH, Hong SI. On the die corner gap formation in equal channel angular pressing. Materials Science and Engineering A. 2000;291(1):86–90.

[21] Basavaraj P. Influence of friction in equal channel angular pressing-a study with simulation. Metal, 2008;13–15(5):1–9.

[22] Patil Basavaraj V. 3D finite element simulation of equal channel angular pressing with different material models. International Journal of Emerging Technologies and Innovative Research, 2016; 3(3):16–28.

[23] Roodposhti PS, Farahbakhsh N, Sarkar A, Murty KL. Microstructural approach to equal channel angular processing of commercially pure titanium—A review. Transactions of Nonferrous Metals Society of China, 2015;25(5):1353–66.

[24] Si J, Wu X, Xia K, Zhang J. Equal Channel Angular Extrusion of TB2 Alloy under Different Die Designs by Finite Element Method. Rare Metal Materials and Engineering, 2014;43(7):1577–81.

[25] Kim WJ, Namkung JC. Computational analysis of effect of route on strain uniformity in equal channel angular extrusion. Materials Science and Engineering A, 2005;412(1–2):287–97.

[26] Tham YW, Fu MW, Hng HH, Yong MS, Lim KB. Study of deformation

homogeneity in the multi-pass equal channel angular extrusion process. Journal of Materials Processing Technology, 2007;192–193:121–7.

[27] Al-Mufadi F, Djavanroodi F. Finite Element Modeling and Mechanical Properties of Aluminum Proceed by Equal Channel Angular Pressing Process. International Journal of Materials and Metallurgical Engineering, 2014;8(8):1402–7.

[28] Fu MW, Tham YW, Hng HH, Lim KB. The grain refinement of Al-6061 via ECAE processing: Deformation behavior, microstructure and property. Materials Science and Engineering A, 2009;526(1–2):84–92.

[29] Mahallawy N El, Shehata FA, Hameed MA El, Aal MIA El, Kim HS. 3D FEM simulations for the homogeneity of plastic deformation in Al-Cu alloys during ECAP. Materials Science and Engineering A, 2010;527(6):1404–10.

[30] Howeyze M, Arabi H, Eivani AR, Jafarian HR. Strengthening of AA5052 aluminum alloy by equal channel angular pressing followed by softening at room temperature. Materials Science and Engineering A, 2018;720:160–8.

[31] Hashimoto S, Suzuki T, Vinogradov A. Hardening Mechanisms of Metals and Alloys Produced by SPD. Materials Science Forum, 2006;503–504:967–70.